ORIGINAL ARTICLE

# Antibacterial and antioxidant properties of hesperidin: β-cyclodextrin complexes obtained by different techniques

Andreia Corciova · Constantin Ciobanu · Antonia Poiata ·
Cornelia Mircea · Alina Nicolescu · Mioara Drobota ·
Cristian-Dragos Varganici · Tudor Pinteala · Narcisa Marangoci

**Abstract** The purpose of this study was to investigate the influence of β-cyclodextrin on aqueous solubility of hesperidin. The inclusion complexes were prepared by different methods (kneading, co-evaporation and lyophilization) and were tested for their antimicrobial and antioxidant activities. Solubility diagrams were drawn at four temperatures (20, 25, 37 and 40 °C) and the corresponding stability constants were calculated. The solubility diagrams obtained were of $A_L$ type and the stoichiometric ratio was 1:1. Moreover, the thermodynamic parameters of the complexation reaction were calculated: Gibbs free energy change, free energy change, enthalpy change and entropy change. The results showed that the complexation reaction is more effective with the increase in temperature and in cyclodextrin concentration. The inclusion process is endothermic and spontaneous and the interactions between hesperidin and β-cyclodextrin are hydrophobic. UV–Vis, FTIR, ¹HNMR, methods provided valuable information about complex formation. Antibacterial activity was investigated by the agar diffusion method, against *Staphylococcus aureus* ATCC 25923, *Escherichia coli* ATCC 25922 and *Candida albicans* ATCC 10231. The results revealed that all the prepared compounds display a higher antibacterial activity compared to hesperidin. Also, the inclusion compounds presented an improved antioxidant activity, demonstrated by the determination of inhibition of lipoxygenase activity, DPPH radical scavenging activity and determination of reducing capacity. In vitro dissolution tests demonstrated that the inclusion compounds have an improved dissolution, compared to free hesperidin. The enhancement in the solubility, antibacterial and antioxidant activities depend on the method of preparation.

**Keywords** Hesperidin · β-cyclodextrin · Inclusion complex · Antibacterial capacity · Antioxidant capacity · In vitro dissolution profile

## Introduction

Hesperidin (HES) (Fig. 1a) is a naturally occurring flavanone glycoside which is found in citrus peel, used alone or in combination, as vascular-protecting agents, for treating chronic venous insufficiency, hemorrhoids, lymphedema, and varicose veins [1]. The HES presents antioxidant and anti-inflammatory properties [2], anti-proliferative and anti-cancer properties [3]. Also, HES significantly decreases the cholesterol levels, total lipids and triglycerides and may be used in the prevention of atherosclerosis and hypertension diseases [4]. Likewise, HES decreases the bone density loss [5] and manifests antinociceptive and sedative activity [6]. Due to its poor solubility in water, the administration is rather limited.

In this context, complexation of insoluble drugs with cyclodextrins, offers, without changing their original structures, the possibility to improve their aqueous solubility, stability to light and oxygen or smell removing, and may allow homogeneous drug delivery systems, increasing their bioavailability [7–11].

Cyclodextrins are cyclic oligosaccharides and are usually formed by 6, 7 or 8 glucose units, covalently bounded

A. Corciova · C. Ciobanu · A. Poiata · C. Mircea · T. Pinteala
"Grigore T. Popa" University of Medicine and Pharmacy Iasi,
Iasi, Romania

A. Nicolescu · M. Drobota · C.-D. Varganici · N. Marangoci (✉)
"Petru Poni" Institute of Macromolecular Chemistry, 41A
Grigore Ghica-Voda Alley, 700487 Iasi, Romania
e-mail: nmarangoci@icmpp.ro

**Fig. 1** Chemical structure of
HES (**a**) and β-CD (**b**)
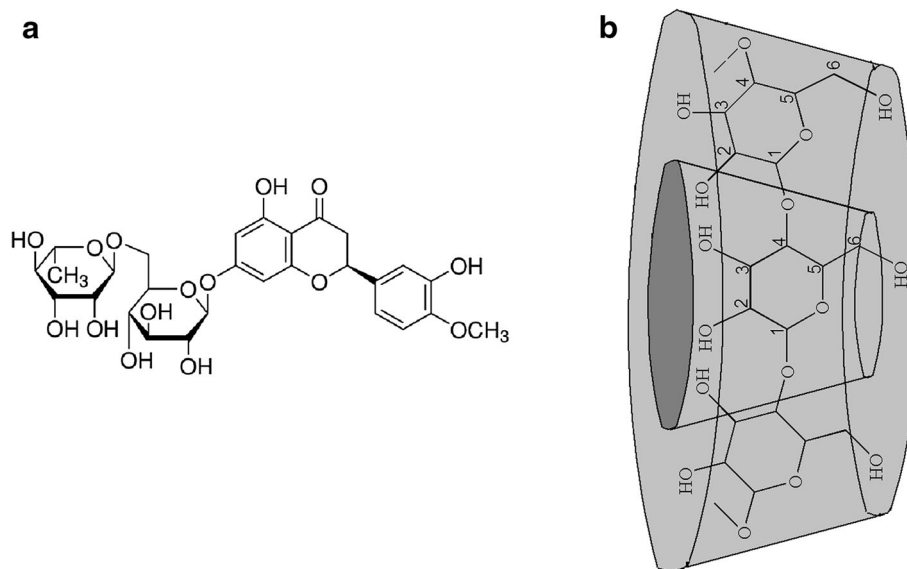


by α-1,4 linkages, named α-, β-, or γ-cyclodextrins,
respectively. Due to their hydrophilic exterior and their
truncated cone hydrophobic interior, they can form host–
guest inclusion complexes with small molecules or parts of
insoluble drug molecules [8, 9, 11, 12].

Due to the important pharmacological properties of
HES, the emphasis of this work was to synthesize com-
plexes of HES with β-cyclodextrin (β-CD) (Fig. 1b) by
different techniques (kneading, co-evaporation and lyoph-
ilization) in order to study their properties and to test an
improved homogenous delivery system for the antibacterial
and antioxidant properties. The characterization of the
complex formation was investigated using FTIR, $^1$HNMR
and DSC methods. The solubility studies were investigated
by determining the phase solubility at different tempera-
tures (20, 25, 37 and 40 °C) and different concentrations of
β-CD in supersaturated water solutions of HES.

We did not realize solubility tests at temperatures above
40 °C, because we were interested in the stability of the obtained
complex at temperatures similar to physiological conditions.

The content of HES in water was determined by UV
spectrophotometry. In addition to the stability constants,
the thermodynamic parameters of the complexation reac-
tion, such as: Gibbs free energy change ($\Delta G_{tr}^0$), free energy
change ($\Delta G^0$), enthalpy change ($\Delta H^0$) and entropy change
($\Delta S^0$) were determined.

## Materials and methods

### Materials

Hesperidin (HES) was purchased from Sigma Aldrich
(USA), having the following characteristics: hesperidin

(HES) ((2S)-5-hydroxy-2-(3-hydroxy-4-methoxyphenyl)-7-
[(2S,3R,4S,5S,6R)-3,4,5-trihydroxy-6-[[(2R,3R,4R,5R,6S)-
3,4,5-trihydroxy-6-methyloxan-2-yl]oxymethyl]oxan-2-
yl]oxy-2,3-dihydrochromen-4-1), ≥80 %, CAS number
520-26-3, molar mass 610.56 g mol$^{-1}$, molecular formula
$C_{28}H_{34}O_{15}$. The β-cyclodextrin (β-CD) was purchased from
Sigma Aldrich (USA), CAS Number 7585-39-9, empirical
formula $C_{42}H_{70}O_{35}$, molecular weight 1,135 g mol$^{-1}$. All
other used reagents were of analytical grade.

### Methods

#### Phase solubility studies

Phase solubility studies were conducted according to the
Higuchi and Connors method [13]. In brief: over the
same volumes of supersaturated water solution of HES
were added the same volumes of different concentrations
of β-CD water solutions (1.0–16.0 mM). The mixtures
were stirred for 24 h, then the unreacted HES was
removed through filtering, using a 0.45 μm, nylon disc
filter. The concentration of HES was determined spec-
trophotometrically by measuring the absorbance of sam-
ples at 286 nm against a blank containing β-CD. Phase
solubility studies were realized at different temperatures,
20, 25, 37 and 40 ± 1 °C [16]. The phase solubility
diagram was drawn by plotting the concentration of HES
versus the concentration of β-CD at different tempera-
tures [8, 14–16]. All samples were analyzed in triplicate.
The concentration of HES in each solution was deter-
mined using suitable constructed standard curves. The
apparent stability constant ($K_S$) was calculated, according
to equation 1.

$$Ks = \frac{slope}{S_0 (1 - slope)} \qquad (1)$$

where: slope—was calculated from the graph; $S_0$—was intrinsic solubility of HES in the absence of β-CD. The dissociation constants, $K_d$, has been assessed trough the equation 2 [14].

$$Kd = \frac{1}{Ks} \qquad (2)$$

### Preparation of inclusion compounds

The inclusion compounds were prepared by kneading, co-evaporation and lyophilization, using a molar ratio HES:β-CD = 1:1.

– Kneading (KN) method: a suitable quantity of water was added to HES and β-CD powders and the resulted mass was stirred until the water was evaporated [17–20].
– Co-evaporation (CV) method: in a clear saturated water solution of β-CD, at room temperature and under stirring, a solution of HES in ethanol was added dropwise. The mixture was stirred for 24 h at 30 °C and after that the temperature was decreased at room temperature, under continuous stirring, until the solvent was evaporated. The homogeneous paste was dried at 40 °C until constant weight [18, 19].
– Lyophilization (L): over a clear β-CD saturated water solution, HES was added under stirring. The resulting suspension was vigorously stirred for 72 h at room temperature, was frozen at −40 °C and then the water was removed by vacuum sublimation [11, 20].

In order to demonstrate the inclusion complexes' formation, the prepared compounds must be characterized. For this purpose, the literature provides us with various techniques, such as: UV–Vis spectroscopy [11, 19, 21, 22], FT-IR [17, 18], ¹HNMR [19, 23], Differential scanning calorimetry [11, 18–20, 23, 24].

### Physico-chemical inclusion compounds characterization

Our conditions of analysis for physico-chemical inclusion compounds characterization were:

– UV–Vis measurements were performed using a double beam Jasco UV–Vis 530 spectrophotometer the measurements were made in 1.0 cm quartz cells at a scan speed of 1,000 nm min⁻¹, fixed slit width of 2 nm and scan range of 200–400 nm.
– Fourier transform infrared spectroscopy (FTIR) spectra for HES, β-CD and their inclusion compounds were obtained using a Bruker Vertex 70 device, equipped with ATR device (Golden Gate, Bruker) via Attenuated

Total Reflectance (ATR) technique. The absorptions were measured in a wavenumber range from 4,000 to 500 cm⁻¹. For a spectrum, 64 scans were taken, with a baseline correction.
– ¹HNMR spectra were obtained using a DRX 400 Avance Bruker 400 MHz spectrometer.
– Differential scanning calorimetry (DSC) measurements were conducted on a DSC 200 F3 Maia device (Netzsch, Germany). About 10 mg of each sample were heated in pressed and pierced aluminum crucibles. A heating rate of 10 °C min⁻¹ was applied. Nitrogen purge gas was used as inert atmosphere at a flow rate of 50 mL min⁻¹. The device was calibrated for temperature and sensitivity with indium, according to standard procedures.

### Antimicrobial activity

The qualitative antimicrobial assay of the samples was carried out by the agar diffusion method [25, 26]. The method can be useful for the initial screening of the compounds' antimicrobial activity. The test organisms were *Staphylococcus aureus (S. aureus)* ATCC (American Type Culture Collection) 25923, *Escherichia coli (E. coli)* ATCC 25922 and *Candida albicans (C. albicans)* ATCC 10231. The antimicrobial tests were carried out using a suspension containing the overnight culture of bacteria ($\sim 10^8$ cfu/ml) and yeast ($\sim 10^7$ cfu/ml). The cultures were inoculated in soft Mueller–Hinton agar (for bacteria) and Sabourand maltose agar medium (for *C. albicans*). The molten agar containing the microbial culture was transferred in a sterile Petri dish. Wells of 6 mm in diameter were placed on the surface of previously seeded agar plates and were filled with 100 µl inclusion compounds, DMSO solvent and with free HES. The bacterial growth inhibition zones around wells were measured after overnight incubation at 37 °C. Each microorganism was tested in triplicate.

### Antioxidant activity

In vitro antioxidant activity of the prepared compounds versus HES and β-CD was evaluated by three methods: determination of the inhibition of lipoxygenase activity (modified Malterud method), 2, 2 diphenyl-picryl-hydrazyl (DPPH) radical scavenging activity and determination of the reducing capacity.

– *Method 1:* The determination of the inhibition of lipoxygenase activity consists in the ability of HES and its inclusion compounds to block the action of lipoxygenase which catalyses the oxidation of linoleic acid with the reduction in absorbance at 234 nm [27].

0.05 mL of pH 9 borate buffer lipoxygenase was treated with 0.05 mL sample solution in DMSO, then, after 10 min at room temperature 2 mL of linoleic acid in 0.16 mM borate buffer pH 9 were added. The absorbance was recorded at 234 nm in the range 0–120 s. The ability to inhibit the lipoxygenase activity was calculated according to equation 3:

$$\% \text{ activity } = \frac{(A_E - A_{EI})}{A_E} \times 100 \qquad (3)$$

where $A_E$ is the difference between the absorbance of the enzyme without inhibitor at second 90 and the absorbance of the same solution at second 30; $A_{EI}$ is the difference between the absorbance of the enzyme with inhibitor at second 90 and the absorbance of the same solution at second 30.For each sample the $IC_{50}$ value was calculated, expressed in mM HES in final solution.

– *Method 2*: Determination of free radicals scavenger activity—DPPH assay: The principle of this method is that the reducing compounds are capable to neutralize the DPPH radical (purple) to diphenyl-picrazine (yellow) with a progressive reduction of the absorbance at 517 nm [28, 29]. 0.3 mL sample (in DMSO) was treated with 2.7 ml of 4 mg % DPPH methanolic solution and after 10 min the absorbance's degree of decrease was determined at 517 nm. The scavenger activity was calculated according to equation 4:

$$\% \text{ scavenger activity } = \frac{(A_{DPPH} - A_{DPPH-S})}{A_{DPPH}} \times 100 \qquad (4)$$

where $A_{DPPH}$ is the DPPH Absorbance; $A_{DPPH-S}$ is the DPPH Absorbance treated with sample after 10 min.- For samples that achieved 50 % scavenger capacity the $IC_{50}$ value was calculated.

– *Method 3*: Determination of the reducing capacity: This method is based on the ability of the substances to reduce the potassium ferricyanide to potassium ferrocyanide which reacts with the ferric ion to form a blue colored complex with maximum absorbance at 700 nm. For this purpose the sample solution was treated with pH 6.6 phosphate buffer and 1 % potassium ferricyanide. The mixture was maintained for 20 min at 50 °C, cooled, treated with 10 % trichloroacetic acid, after which the supernatant was separated and treated with 0.1 % $FeCl_3$ and the absorbance was recorded at 700 nm [30]. For samples where the final solution absorbance was above 0.5, the $IC_{50}$ value was determined. The reducing capacity was calculated based on a formula that uses the absorbance and the concentration of the solutions that showed the absorbance just under 0.5 and over 0.5.

### In vitro dissolution studies

In vitro dissolution studies of HES and its inclusion compounds with β-CD were carried out using an USP paddle apparatus. Samples containing the same amount of HES (free and from inclusion compounds) were transferred in dissolution medium (0.1 N hydrochloric acid solution—simulated gastric fluid pH 1.2 and phosphate buffer—simulated intestinal fluid pH 6.8), stirring speed 100 rpm at a temperature of 37 ± 0.5 °C. 5 ml of samples were withdrawn at time intervals of 10, 20, 30, 40, 60, 90 and 120 min, by replacing each withdrawn aliquot with the same volume of dissolution medium. Each sample was filtered and then the HES concentration was determined by UV measurements at 286 nm against a blank containing the used medium. The concentration of HES in each solution was determined with reference to a suitable constructed standard curve. Dissolution studies were performed in triplicate. The dissolution diagrams were drawn by plotting mean values of cumulative dissolution of HES versus time [31, 32].

## Results and discussion

### Phase solubility studies

Figure 2 shows the UV–Vis spectra and the solubility curves obtained for HES in the presence of β-CD in distilled water at different temperatures (20, 25, 37 and 40 °C). The interactions of HES and β-CD can be examined by comparing the UV–Vis spectra of free HES and in the presence of β-CD in water solutions (Fig. 2a).

Free HES exhibits an intense maximum at 284 nm and a shoulder at 328 nm, demonstrating the presence of different phenyl rings, due to their $\pi \rightarrow \pi^*$ electronic rearrangement and to the $n \rightarrow \pi^*$ electronic transition of an electron from a n non-bonding molecular orbital to a $\pi^*$ anti-bonding molecular orbital, characteristic for the C=O bond [33, 34]. From the UV–Vis spectra of HES in the presence of different β-CD concentrations, modifications in the absorbance values and bathocromic effects (when the wavelength maximum values are shifted from 284 to 286 nm and from 328 to 330 nm) were observed. These modifications can indicate the possibility of inclusion complex formation. As it can be seen for each temperature, the solubility of HES in water presented a linear growth when the CD concentration increased. The resulting linear curves can be classified, in general, as an $A_L$ type (linear positive isotherm), and since the slopes of the diagrams were less than one (Table 1) it was assumed that the stoichiometry of each complex was 1:1, according to Higuchi and Connors [13]. It should be noted that the solubility of

**Fig. 2** UV-Vis spectra of HES versus β-CD concentration (**a**), phase solubility diagrams of HES in water solutions versus β-CD concentration at 20, 25, 37 and 40 ± 1 °C (**b**). *Inset* HES etalon curves in water at 20, 25, 37 and 40 ± 1 °C
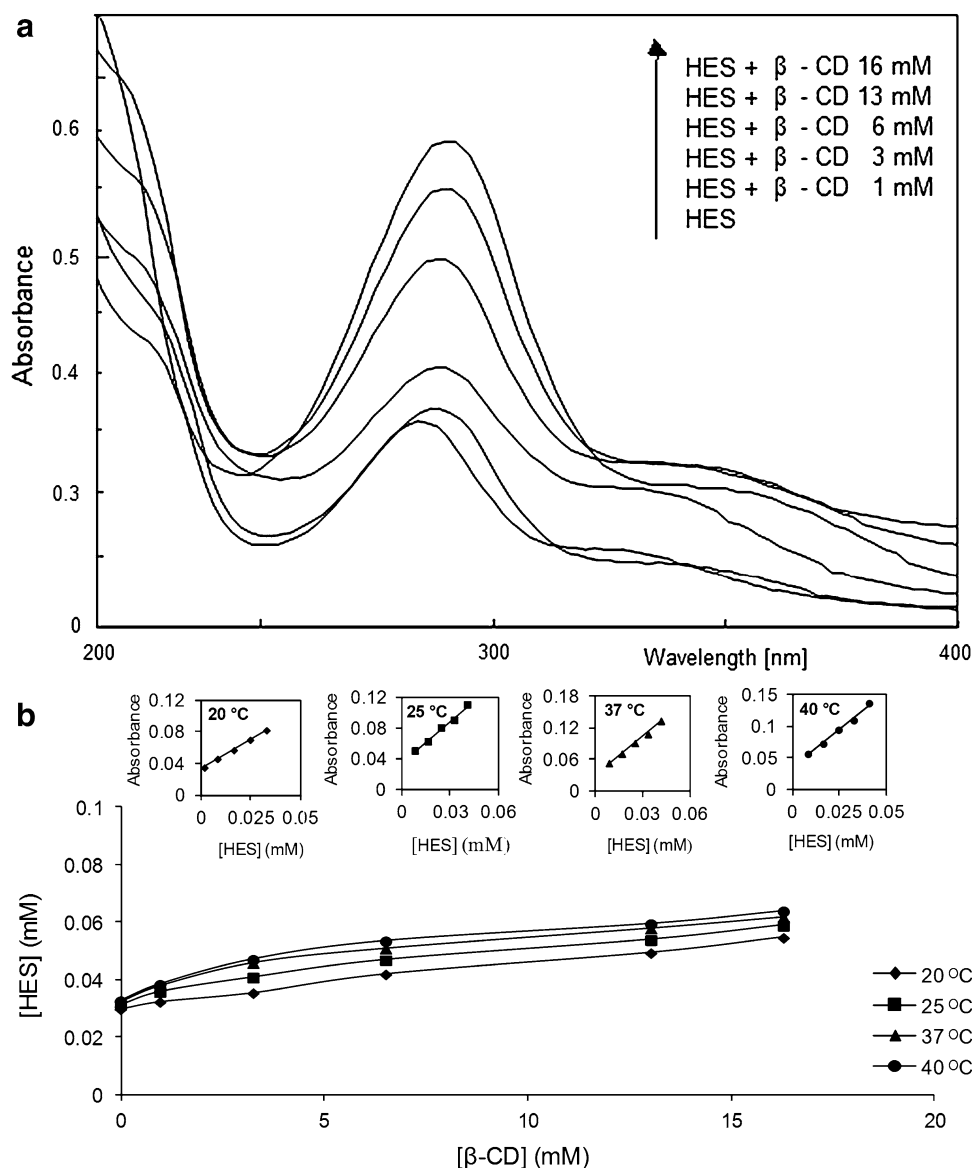


**Table 1** $K_s$ and $K_d$ values of HES:β-CD complex in water at different temperatures

| Temperature (°C) | slope | Ks (M$^{-1}$) | Kd (M) |
|---|---|---|---|
| 20 | 0.0049 | 153.87 | 0.0065 |
| 25 | 0.0055 | 172.82 | 0.0057 |
| 37 | 0.0062 | 194.95 | 0.0051 |
| 40 | 0.0063 | 198.73 | 0.0050 |

HES in the presence of β-CD was increasing. The binding or association constants at different temperatures ($K_s$, M$^{-1}$) of the complex in water were calculated from the correspondent curves of Fig. 2b, according to equation 1 (for dissociation constants according to equation 2), and were found to be in range of 153.87–198.73 M$^{-1}$ (Table 1), demonstrating that the process is favorable to obtain

inclusion compounds. It is known that the optimal values for the stability constants are included in the range of 100–1,000 M$^{-1}$ [16, 35].

In the formation of complexes the thermodynamic interactions between the various components of the system (cyclodextrin, substance, solvent) are critical factors. In order to form a complex, a favorable energy is needed to push the substance into the cyclodextrin cavity, and the change of temperature influences the complexation between the substance and cyclodextrin. In view of these facts, in addition to the stability constants, we have determined the thermodynamic parameters of the complexation reaction, such as: Gibbs free energy change, free energy change, enthalpy change and entropy change.

Using the data from Fig. 2, the Gibbs free energy change ($\Delta G_{tr}^0$, kJM$^{-1}$) can be calculated using equation 5, indicating the transfer of HES from water in the β-CD

**Table 2** $\Delta G_{tr}^0$, $\Delta G^0$ values (kJM$^{-1}$), for HES depending on temperature and β-CD concentration

|  | β-CD (mM) | Temperature | | | |
|---|---|---|---|---|---|
|  |  | 20 °C (293 K) | 25 °C (298 K) | 37 °C (310 K) | 40 °C (313 K) |
| $\Delta G_{tr}^0$ (kJM$^{-1}$) | 1.0 | −0.080 | −0.194 | −0.265 | −0.279 |
|  | 3.0 | −0.182 | −0.335 | −0.471 | −0.504 |
|  | 6.0 | −0.352 | −0.520 | −0.633 | −0.645 |
|  | 13.0 | −0.524 | −0.584 | −0.728 | −0.764 |
|  | 16.0 | −0.632 | −0.722 | −0.801 | −0.845 |
| $\Delta G^0$ (kJM$^{-1}$) |  | −12.146 | −12.638 | −13.585 | −13.635 |

microenvironment [16]. Also, the Gibbs free energy change (Table 2) will provide data regarding favorable or unfavorable conditions concerning the solubility of HES in β-CD solution.

$$\Delta G_{tr}^0 = - RT \log \frac{S}{S_0} \qquad (5)$$

where $\Delta G_{tr}^0$ is the Gibbs free energy change (kJM$^{-1}$); R is the gas constant (JM$^{-1}$K$^{-1}$); T is the absolute temperature of the reaction (K); $S/S_0$ = was the ratio between the solubility of HES in β-CD water solution and the solubility of HES in water.

Knowing the equilibrium constant and the temperature at which the measurements were made (Table 1), the standard deviation of the Gibbs free energy ($\Delta G^0$, kJM$^{-1}$) to the equilibrium constant can be determined (Table 2), according to equation 6 [14–16, 22, 36].

$$\Delta G^0 = -2.303 \ RT \log K_s \qquad (6)$$

where: $\Delta G^0$ is the Gibbs free energy (kJM$^{-1}$); R = the gas constant (JM$^{-1}$K$^1$); T is the absolute temperature of the reaction (K); $K_s$ is the equilibrium constant of the complex formed with 1:1 stoichiometry (M$^{-1}$).

Regarding our results from Table 2, the negative values of $\Delta G_{tr}^0$ indicate favorable conditions for the solubilization of HES in the presence of β-CD. These values decrease with the increasing of the β-CD concentration and the temperature of the process, which demonstrates that the reaction becomes more favorable with the increasing of the β-CD concentration and the temperature of the sample.

From Table 2 it can be observed that the values of $\Delta G^0$ are negative, proving that the inclusion process evolves spontaneously at the chosen temperatures [15, 16, 22, 35, 37].

Furthermore, calculating the changes in the entropy ($\Delta S^0$, JM$^{-1}$) and enthalpy ($\Delta H^0$, kJM$^{-1}$), information about the strength of the interaction between HES and β-CD can be obtained. The enthalpy change ($\Delta H^0$, kJM$^{-1}$) was determined from the slope (equation 7) of the line

resulted by the representation of log $K_s$ versus 1/T according to the van't Hoff equation (equation 8) [15, 16, 22, 38]. The standard entropy change ($\Delta S^0$, JM$^{-1}$) for the complexation reaction was calculated using the equation 9, for each temperature [16, 20].

$$\text{Slope} = \frac{\Delta H^0}{2.303R} \qquad (7)$$

where: Slope is the slope of log Ks versus 1/T line graph; $\Delta H^0$ is the enthalpy change (kJM$^{-1}$); R is the gas constant (JM$^{-1}$K$^{-1}$)

$$\log K_s = - \frac{\Delta H^0}{RT} + \frac{\Delta S^0}{R} \qquad (8)$$

where: $K_s$ is the equilibrium constant of the complex formed with 1:1 stoichiometry (M$^{-1}$); $\Delta H^0$ is enthalpy change (kJM$^{-1}$); R is the gas constant (JM$^{-1}$K$^{-1}$); $\Delta S^0$ is the entropy change (JM$^{-1}$); T is the absolute temperature of the reaction (K).

$$\Delta G^0 = \Delta H^0 - T\Delta S^0 \qquad (9)$$

where: $\Delta G^0$ is the Gibbs free energy (kJM$^{-1}$); $\Delta H^0$ is the enthalpy change (kJM$^{-1}$); T is the absolute temperature of the reaction (K); $\Delta S^0$ is the entropy change (JM$^{-1}$).

In our case $\Delta S^0 = 43.94$–$45.89$ (JM$^{-1}$) and $\Delta H^0 = 0.731$(kJM$^{-1}$) were calculated, demonstrating that the inclusion complex formation is an endothermic process given by positive value of $\Delta H^0$ and the transfer of HES from aqueous medium into the β-CD is realized by hydrophobic interactions due to the positive value of $\Delta S^0$ [16].

## Physico-chemical characterization of HES:β-CD inclusion complexes obtained by different techniques

### Fourier transform infrared spectroscopy (FTIR)

The FTIR spectra of HES, β-CD and their complexes obtained by different techniques are presented in Fig. 3. IR spectroscopy can provide information on the formation of complexes because the specific absorption bands of the free components are generally shifted or their intensities are modified [39]. When the spectra were analyzed, the FTIR spectra of the complexes obtained by different techniques were very similar but different from FTIR spectra of HES and β-CD. In the β-CD FTIR spectrum, the wide absorption band with maximum at 3,325 cm$^{-1}$ (O–H stretching vibrations) was present. Also, there were other characteristic bands at 2,926 cm$^{-1}$ (CH and CH$_2$ aliphatic), 1,645 cm$^{-1}$ (OH groups of the glucopyranosyl unit [40], 1,400–1,300 cm$^{-1}$ (CH deformation vibrations) and at 1,030–1,082 cm$^{-1}$ (C–O–C and C–OH stretching vibrations [41]. In the FTIR spectrum of HES, the characteristic

absorption bands were present at 3,403 and 3,534 cm$^{-1}$ (OH stretching vibrations), 2,919 cm$^{-1}$ (CH and CH$_2$ aliphatic), 1,645 and 1,607 cm$^{-1}$ (C=O in ketones) and at 1,605, 1,594, 1,576 cm$^{-1}$ (C=C valence vibrations in the benzene rings). The absorption bands in 950–700 cm$^{-1}$ interval are specific for the pulsation vibrations in glucopyranosyl unit and deformation vibrations of C–H bonds [40]. In the FTIR spectra of the complexes (Fig. 3) few differences exist if we compare to those of HES and β-CD. Concerning the 1,800–1,500 cm$^{-1}$ interval (insert of Fig. 3), a new shoulder at 1,733 cm$^{-1}$ was observed due to the presence of HES into cyclodextrin cavity. The vibration absorption bands of the C–O–C bonds in the range 1,200–1,030 cm$^{-1}$ are extended in the inclusion complex as compared to HES and β-CD spectra. Furthermore, the absorption bands of the C=C bonds from phenyl rings of HES are slightly shifted at 1,609, 1,593 and 1,574 cm$^{-1}$ (insert of Fig. 3). The deconvolution of the FTIR spectrum of β-CD in the range of 3,700–3,000 cm$^{-1}$ shows 9 peaks (Fig. 4a) at 3,558 cm$^{-1}$ attributed to OH from the hydrophobic β-CD cavity and the other peaks are cased by valence vibrations of intermolecular bonds of primary hydroxyls (3,500 and 3,448 cm$^{-1}$) and intramolecular bonds of secondary hydroxyl groups (3,379, 3,310, 3,248, 3,130, 3,194, 3,064 cm$^{-1}$) [39]. The deconvolution of the FTIR spectrum of HES (Fig. 4b) presents two deconvoluted bands (3,293, 3,251 cm$^{-1}$) of the hydroxyls connected to phenyl rings, 2 bands (3,542 and 3,452 cm$^{-1}$) attributed to the intermolecular bonds of primary hydroxyls and 6 bands of intramolecular secondary hydroxyls of the glucopyranosyl units. The fitting curves of the FTIR spectra of the complexes obtained by different techniques are similar and the disappearance of the band of OH groups from β-CD cavity was observed. The complexes (Fig. 4c) presented four shifts of lower intensity in the fitting curves at 3,416, 3,320, 3,221, 3,083 cm$^{-1}$ due to the intermolecular bonds of primary hydroxyls and intramolecular secondary hydroxyls of the glucopyranosyl units. In addition, the complexes presented an up-shifted peak at 3,253 cm$^{-1}$ and an down-shifted peak at 3,201 of the hydroxyl groups connected to the different phenyl rings. The intense peak at 3,462 cm$^{-1}$ was attributed to the stretching vibrations, at high-frequency, of the C=O group at 1,731 cm$^{-1}$ ($2 \times 1,731 = 3,462$ cm$^{-1}$). All these results confirmed the formation of the inclusion complex between β-CD and HES by any method of preparation.

## $^1$H-NMR spectroscopy

Analyzing the chemical structure of HES (Fig. 1a) we can suppose the formation of two types of inclusion complexes with a more or less probability, depending on the organic radical of HES, hydroxy-methoxyphenyl part and

glucopyranosyl unit, respectively. It should be noted that studying the inclusion phenomenon of a drug into the cyclodextrin cavity, shifts of H$_3$ and H$_5$ of β-CD should be observed [11, 42–44]. In our case, due to the presence of glucopyranosyl units in both components (drug and β-CD) which are responsible for the inclusion complex formation, those shifted peaks are undistinguishable. Moreover, it is unlikely that the hydrophilic glucopyranosyl unit of HES to penetrate the hydrophobic cavity of CD, therefore we considered the shifts of the methoxy, CH$_2$, CH and phenyl protons of HES for further studies. The $^1$H-NMR spectra of β-CD, as a function of HES concentration, are shown in Fig. 5 (in ppm). It can be observed small shifted $^1$H-NMR signals of methoxy and phenyl protons from -Ph-OCH$_3$ radical of HES between 1:3 to 1:1 molar ratios of HES:β-CD (see also Table 3), while all the other peaks remain almost unchanged, indicating an inclusion phenomenon of the -Ph-OCH$_3$ part into cyclodextrin cavity.

## Differential scanning calorimetry (DSC)

The DSC method offers useful insights on host–guest solid state interactions. By comparing the DSC curves (Fig. 6), one can identify the differences between pure substances and inclusion compounds, differences that may occur by phase transformations after heating.

The complexation phenomenon is generally evidenced by the disappearance or decrease in intensity of the guest molecule melting peak in the inclusion compound. One can observe this aspect in Fig. 6, accompanied by a displacement of the inclusion compounds melting peaks compared to that of the pure uncomplexed guest molecule [41]. In the case of HES, a dehydration peak is observed around 135 °C and the melting peak at 262 °C. β-CD also exhibits an intense and sharp endothermic peak at 145 °C corresponding to loss of crystallized water from its cavity. These two dehydration peaks both appear in the rest of the compounds DSC curves. However, in the case of the three inclusion compounds, the β-CD dehydration peak is strongly reduced in intensity and significantly shifted to the lower temperature domains, with the following values: 113 °C for KN, 120 °C for CV and 118 °C for L. The HES dehydration peak in the inclusion compounds also reduces in intensity without exhibiting significant shifts (133 °C for L, 136 °C for CV and 138 °C for KN) compared to that of free HES dehydration (135 °C). Since HES possesses two glycosidic entities, one must not exclude the possibility of their coupling to the hydrophilic exterior of the β-CD, via OH groups, by hydrogen bonds formation, while the rest of the molecule enters the β-CD cavity demonstrated, also, by $^1$H-NMR and FTIR methods. A significant decrease in the melting peak enthalpy values can be observed for the three inclusion compounds (31.53 Jg$^{-1}$ for L, 35.96 Jg$^{-1}$ for CV

**Fig. 3** FTIR spectra of β-CD (*a*), HES (*b*), CV (*c*), KN(*d*) and L (*e*). *Inset* FTIR spectra of β-CD (*a*), HES (*b*) and CV (*c*) in 1800–1500 cm⁻¹ interval
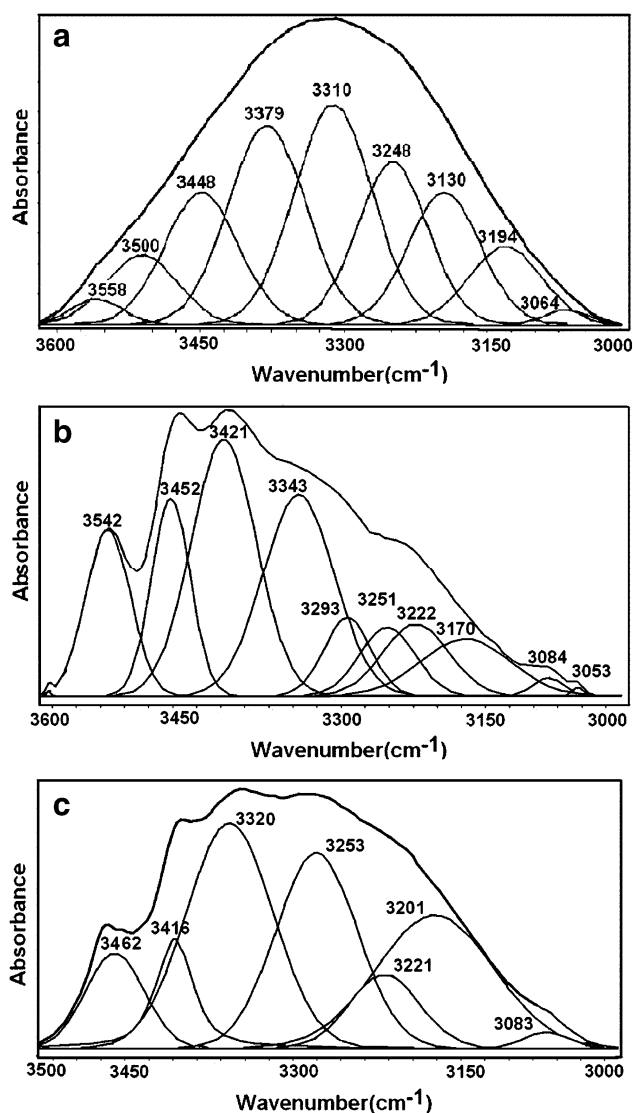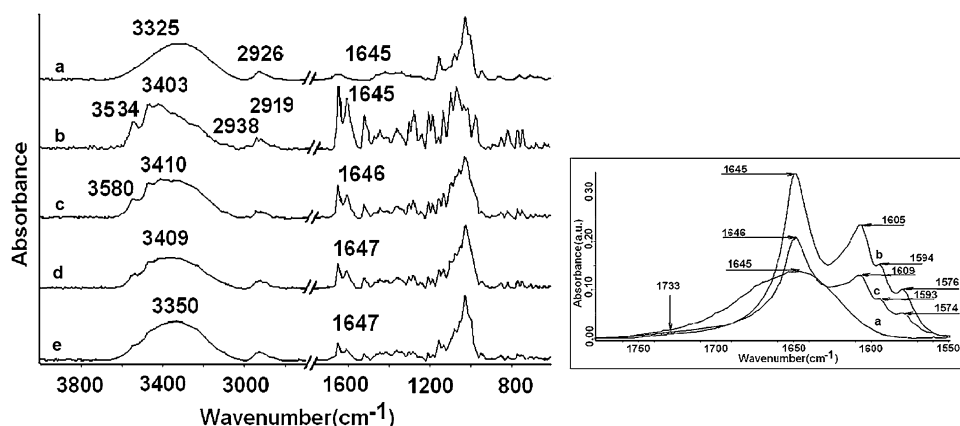




**Fig. 4** Deconvoluted FTIR spectra in 3700–3000 cm⁻¹ interval for the β-CD (**a**), HES (**b**) and CV (**c**)
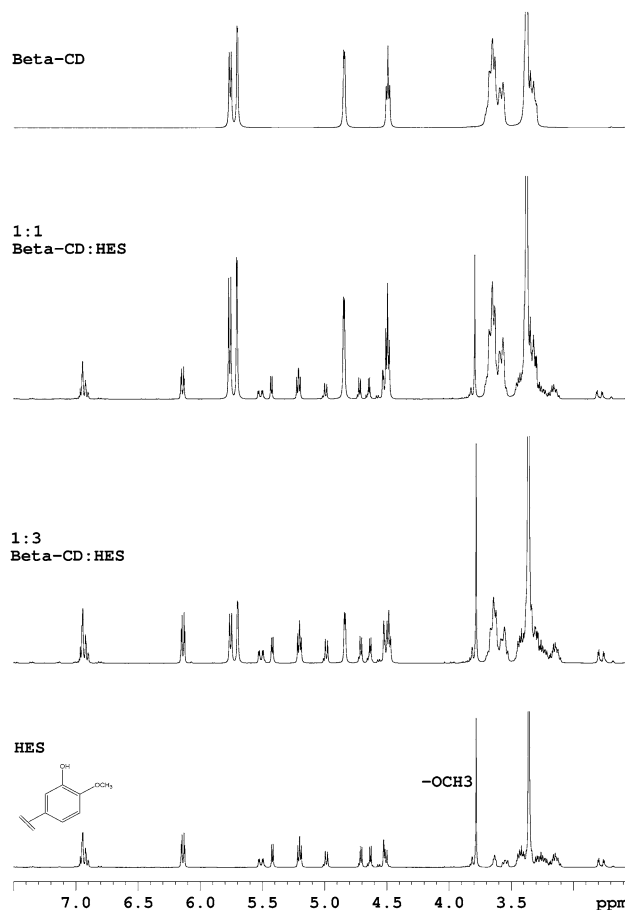


**Fig. 5** ¹HNMR spectra (DMSO$_{d6}$) as a function of molar ratio of β-CD:HES

and 33.8 Jg⁻¹ for KN) and also a slight change in temperature occurred (257 °C for L, 261 °C for CV and 260 °C for KN). These differences also demonstrate the occurrence of complexation phenomenon.

Based on the melting heat values of the inclusion compounds and that of free HES (118.5 Jg⁻¹), an inclusion

**Table 3** $^1$H chemical shifts (δ ppm) of HES, β-CD and their mixture at different molar ratios

| δ (ppm) | HES | β-CD:HES 1:3 | β-CD:HES 1:1 |
|---|---|---|---|
| –OC$\underline{H}_3$ of HES | 3.7822 | 3.7819 | 3.7814 |
| Protons of –Ph-OCH$_3$ of HES | 6.8968–6.9631 | 6.8966–6.9628 | 6.8963–6.9625 |
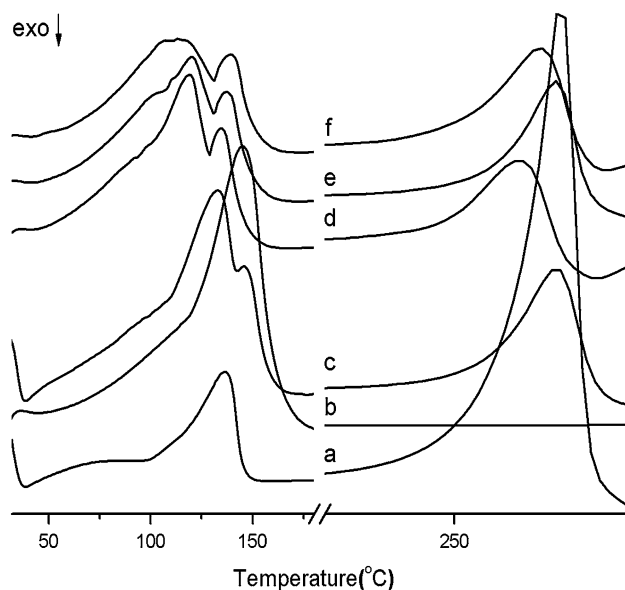


**Fig. 6** DSC curves of HES (*a*), β-CD (*b*), physical mixing (*c*), KN (*d*), CV (*e*) and L (*f*)

efficiency was calculated, by applying equation 10 [45], which decreased in the order: L (73.4 %) > KN (71.5 %) > CV (69.7 %).

$$\% \text{ Inclusion} = \left(1 - \frac{\Delta H_{m1}}{\Delta H_{m2}}\right) \times 100 \qquad (10)$$

where: $\Delta H_{m1}$ is the melting heat value of the inclusion compound (Jg$^{-1}$); $\Delta H_{m2}$ is the melting heat value of the free guest compound (Jg$^{-1}$).

Antimicrobial activity

HES and its β-CD inclusion compounds prepared by kneading, co-evaporation and lyophilization were tested for antimicrobial activity against one Gram (−) *E coli*, one Gram (+) *S. aureus* bacteria and one diploid fungus *C. albicans*, the results being presented in Fig. 7.

Results showed that all the compounds were susceptible to tested organisms and the inclusion compounds displayed a higher antibacterial activity, compared to HES. The tested compounds, obtained by different techniques, presented similar antibacterial activity for *S. aureus* and *E. coli* but a

higher activity was recorded against *C. albicans*. However, some differences in antibacterial activity according to the method of synthesis can be observed; thus, the antibacterial activity decreased in the following order: lyophilization > co-evaporation > kneading. This may be attributed to the enhanced solubility of the inclusion compounds, so HES could be more available for membrane transportation and become more available for specific tissues and could present an increased antibacterial potential [46].

*Antioxidant activity*

The capacity of inhibition of lipoxygenase activity was measured spectrophotometrically at five different concentrations in range 0.5,118–8.189 mM. DPPH radical scavenger activities and reducing capacity were tested at seven different concentrations, in range 0.5,118–32.756 mM, for each sample: kneading, co-evaporation and lyophilization, using as control HES and β-CD.

– *Method 1*. 15-lipoxygenase is an heminic enzyme from oxidoreductases class which is widely distributed in the body. The enzyme is capable of catalyzing the oxidation of unsaturated fatty acids to form lipid peroxides that have high chemical reactivity and can enhance the oxidation reactions of other molecules with biological role, such as proteins, nucleic acids and other lipid compounds [27]. Studies have shown that excessive activity of this enzyme could be involved in the occurrence of pathological processes such as atherosclerosis, diabetes, inflammatory phenomena [47, 48]. Enhanced activity of the enzyme at cerebral level increases the size of amyloid plaques in Alzheimer's disease [49]. Figure 8 presents the capacity of inhibition of lipoxygenase activity for HES, β-CD and their prepared compounds.

The action of the enzyme depends on the oxidation state of the iron ion in the heme structure which is involved in the redox reaction catalyzed by the enzyme. The iron ion blocking is performed by compounds which have reducing hydroxyl groups which will maintain the iron ion only in 2 + oxidation state and thus the transformation of $Fe^{3+}$–$Fe^{2+}$ doesn't occur. The analyzed compounds' lipoxygenase inhibitory effect can be explained through the prevention of the substrate's access (linoleic acid) to the enzyme's active center given the bigger size of the inclusion compounds compared to HES.

– *Method 2*: The DPPH radical scavenging activity expressed in percentage of inhibition of HES, β-CD and their prepared compounds, is presented in Fig. 9. The 2,2-diphenyl-1- picril-hydrazyl radical is reduced (stabilized) using compounds which can yield the

**Fig. 7** Zone of inhibition (mm) for HES and its inclusion compounds with β-CD (obtained by different techniques) on the mentioned bacterial strains
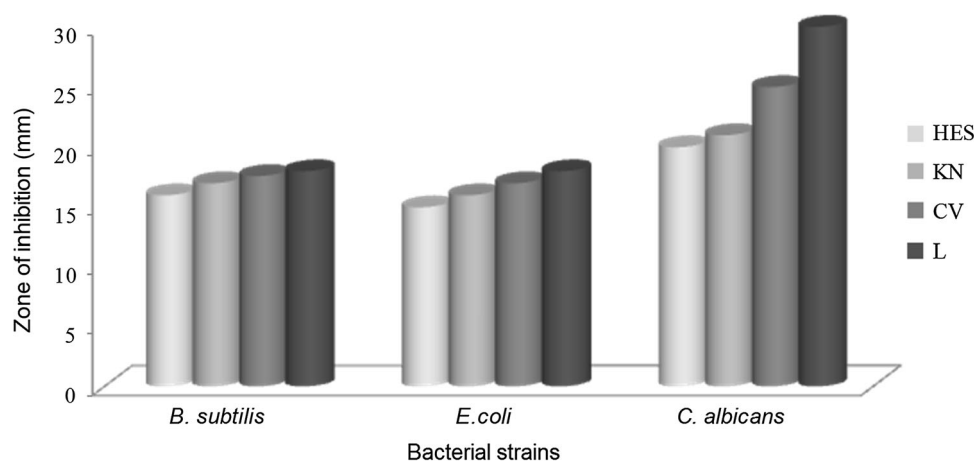


**Fig. 8** The capacity of inhibition of lipoxygenase activity presented by HES, β-CD and their complexes as a function of HES concentration
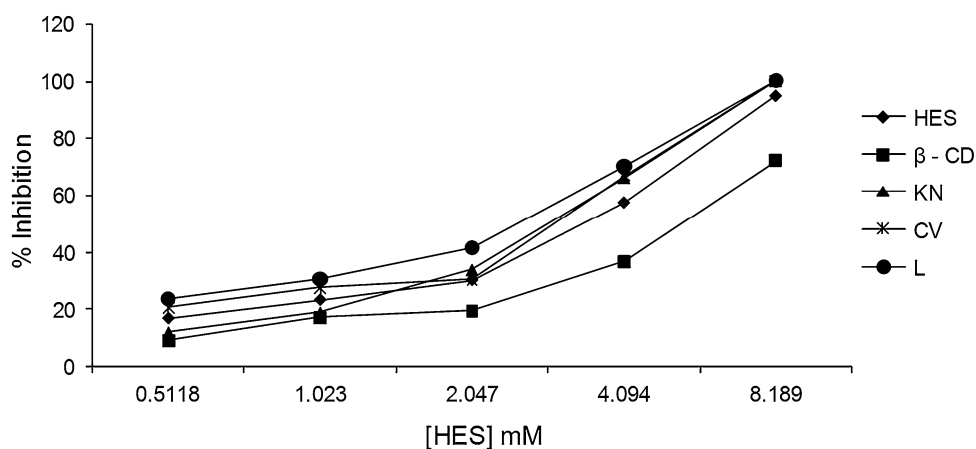


**Fig. 9** DPPH radical scavenging activities of tested compounds, as a function of HES concentration
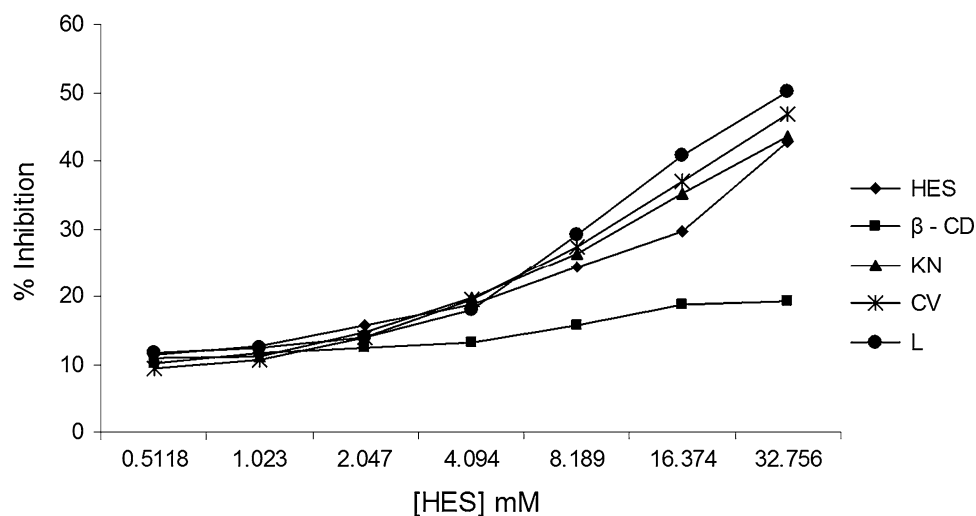


hydrogen atoms of the hydroxyl groups. In this case, both HES and β-CD have OH groups, but hydrogen atoms' mobility is much less than that of other compounds with known reducing properties such as polyphenol carboxylic acids. HES:β-CD inclusion complexes determine the improvement of their reducing properties, but to a lesser extent compared with the observed effects in other antioxidant tests.

– *Method 3*: Reduction of ferric ion to ferrous ion is important in the biological environment because it has

**Fig. 10** Determination of reducing ability of the investigated compounds, as a function of HES concentration
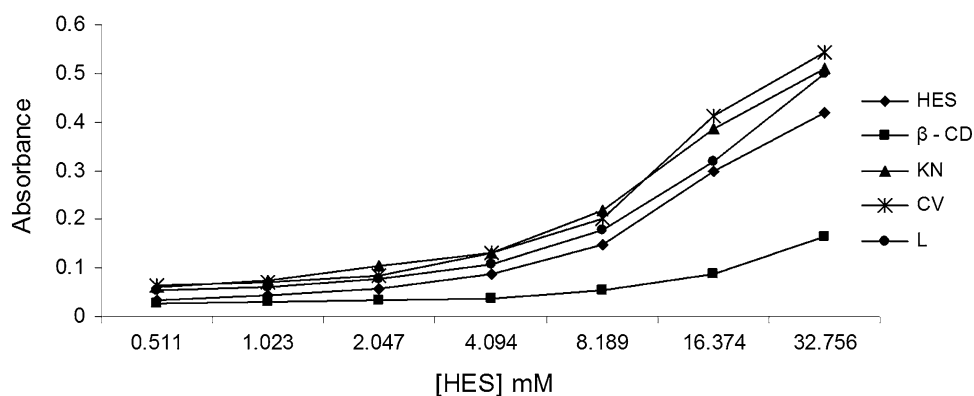


**Table 4** IC$_{50}$ values for the analyzed compounds

| Method/Sample | KN | CV | L | β-CD | HES |
|---|---|---|---|---|---|
| Method 1 (mM) | 0.0484 ± 0.69 | 0.0495 ± 0.66 | 0.0422 ± 0.74 | 0.088 ± 1.40 | 0.0565 ± 0.80 |
| Method 2 (mM) | – | – | 3.233 ± 0,171 | – | – |
| Method 3 (mM) | 3.567 ± 0.016 | 3.123 ± 0.037 | 3.547 ± 0.046 | – | – |

**Fig. 11** In vitro dissolution profile of HES and its inclusion compounds with β-CD in 0.1 N HCl (pH 1.2), depending on time. *Inset* HES etalon curves in 0.1 N HCl
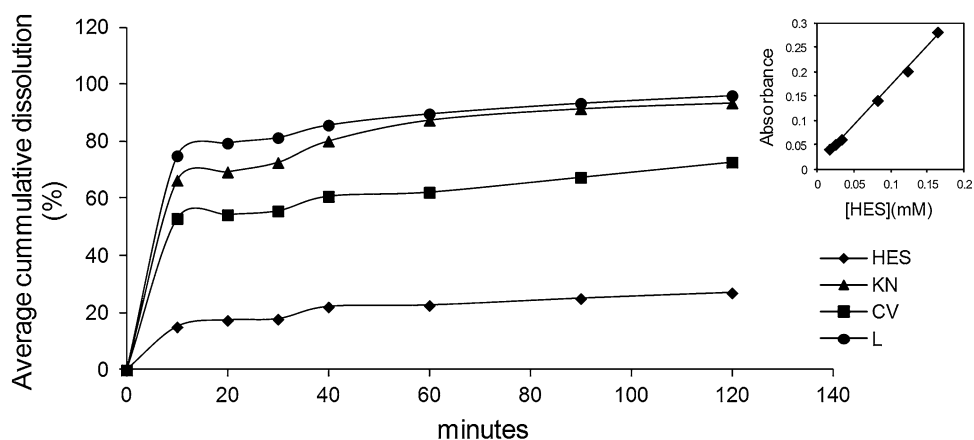


oxidant capacity and causes oxidant species of which the most important are the oxygen reactive species. Figure 10 presents the recorded absorbance depending on samples concentration.

In all cases, determination of the antioxidant activity of the analysed compounds is proportional with their concentration level. The antioxidant activity of the prepared compounds increased after the formation of inclusion compounds, probably due to the increasing solubility of the compounds and therefore increasing the ability to inhibit the lipoxygenase activity, to trap free radicals and to reduce the ferric ions. As it can be observed from Figs. 8 and 10, the samples prepared by lyophilization have the most intensive antioxidant activity (method 1 and 2) and for method 3 by co-evaporation, so the method used for obtaining inclusion compounds influences the antioxidant activity.

Table 3 presents the IC$_{50}$ values calculated by the three used methods and also depending on the inclusion method.

Method 1, as compared with HES and β-CD, KN, CV and L complexes, has better inhibitory activity, as reflected by the lower IC$_{50}$ value Table 4. The use of β-CD determines the improvement of lipoxygenase inhibition exerted by HES.

In method 2, we could calculate the IC$_{50}$ value only for the sample obtained by lyophilization, because for the other samples the maximum concentration taken into work (32.756 mM) did not demonstrate an inhibition greater than 50 %. Thus, we can say that, the antioxidant activity of HES improved after the interaction with β-CD, by this antioxidant method, only in case of lyophilization method.

In method 3, the reduction of ferric ion is performed using proton and electron donor groups such as hydroxyl group, (the HES contains these groups), and in combination

**Fig. 12** In vitro dissolution profile of HES and its inclusion compounds with β-CD in phosphate buffer at pH 6.8, depending on time. *Inset* HES etalon curves in phosphate buffer at pH 6.8
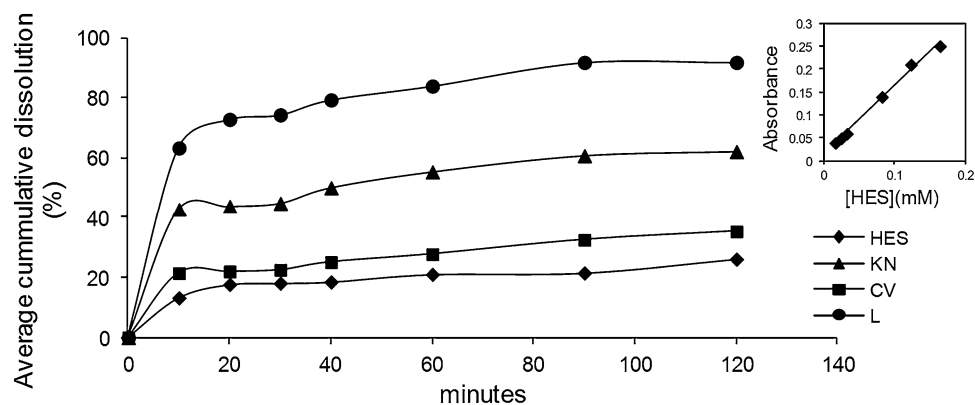
with β-CD, the ability to release electrons and protons is improved, as evidenced by the increase in the reducing capacity compared to the basic compound. For the same concentrations of the basic substances, as in complexes, the 0.5 value of the absorbance was not reached and thus we could not calculate the $IC_{50}$ value. The complexes obtained with β-CD have a better ability to reduce the ferric ion, so for all used methods, the formed complexes gave absorbances over 0.5 which allowed the determination of $IC_{50}$.

### In vitro dissolution studies

In vitro dissolution studies are important in both quality control purposes and drug development because they provide important information about the percent of HES dissolved from inclusion compounds in a specific time and under physiological conditions, like simulated gastric fluid pH 1.2 and simulated intestinal fluid pH 6.8, according to European Pharmacopoeia 7th edition. Figures 11 and 12 present in vitro the % dissolution values of HES in free state and from its inclusion compounds as a function of time and pH values.

From these figures, all inclusion compounds have an improved dissolution [31, 32] as compared to free HES. It should be mentioned that the enhancement in the solubility of HES depends on the method applied in obtaining inclusion complexes; the best dissolution profile was recorded for liophilized sample, followed by kneading and co-evaporation samples.

### Conclusions

In this work we determined the influence of β-CD on the properties of an important flavonoid, HES. The phase solubility diagrams of HES, in aqueous solutions, showed a linear increase in its solubility with increasing the β-CD concentration and the temperature at which the process takes place. The best solubility and stability were obtained at 40 °C, but the difference between 37 and 40 °C is very small. Gibbs free energy change values are negatives and are decreasing with the increasing of the β-CD concentration and the temperature of the process, which demonstrates that the reaction becomes more favorable with the increasing of the β-CD concentration and the temperature of the process. The stability constant was between 153.87 and 198.73 $M^{-1}$ and was slightly influenced by the temperature of the reaction. The values of the thermodynamic parameters confirmed that the inclusion of HES into CD cavity is an endothermic process ($\Delta H^0 = 0.731$ kJM$^{-1}$) and it takes place spontaneously at the chosen temperature. Moreover, the transfer of HES from aqueous medium into the β-CD is realized by hydrophobic interactions due to the positive value of $\Delta S^0$.

The increasing of the HES solubility is attributed to the inclusion complex formation with β-CD, as demonstrated by $^1$H-NMR, FTIR, DSC and UV–Vis methods. The inclusion complexes were obtained in different yield, depending on method of synthesis (kneading, co-evaporation and lyophilization). Furthermore, in vitro studies demonstrated an enhancement of antibacterial, antioxidant and dissolution profiles of inclusion compounds, depending on the method of inclusion, thereby increasing the possibility of using the inclusion compounds in various pharmaceutical preparations in order to improve pharmacological effects.

### References

1. Tong, N., Zhang, Z., Zhang, W., Qiu, Y., Gong, Y., Yin, L., Qiu, Q., Wu, X.: Diosmin alleviates retinal edema by protecting the blood-retinal barrier and reducing retinal vascular permeability during ischemia/reperfusion injury. PLos One **8**, 1–10 (2013)
2. Sezer, A., Usta, U., Kocak, Z., Yagci, M.A.: The effect of a flavonoid fractions diosmin + hesperidin on radiation-induced acute proctitis in a rat model. J. Cancer Res. Ther. **7**, 152–156 (2011)

3. Lee, C.J., Wilson, L., Jordan, M.A., Nguyen, V., Tang, J., Smi-yun, G.: Hesperidin suppressed proliferations of both human breast cancer and androgen-dependent prostate cancer cells. Phytother. Res. **24**, 15–19 (2010)

4. Monforte, M.T., Trovato, A., Kirjavainen, S., Forestieri, A.M., Galati, E.M., Lo Curto, R.B.: Biological effects of hesperidin, a Citrus flavonoid. (note II): hypolipidemic activity on experimental hypercholesterolemia in rat. Farmaco **50**, 595–599 (1995)

5. Chiba, H., Uehara, M., Wu, J., Wang, X., Masuyama, R., Suzuki, K., Kanazawa, K., Ishimi, Y.: Hesperidin, a citrus flavonoid, inhibits bone loss and decreases serum and hepatic lipids in ovariectomized mice. J. Nutr. **133**, 1892–1897 (2003)

6. Loscalzo, L.M., Wasowski, C., Paladini, A.C., Marder, M.: Opioid receptors are involved in the sedative and antinociceptive effects of hesperidin as well as in its potentiation with benzodiazepines. Eur. J. Pharmacol. **580**, 306–313 (2008)

7. Brewster, M.E., Loftsson, T.: Cyclodextrins as pharmaceutical solubilizers. Adv. Drug Deliv. Rev. **59**, 645–666 (2007)

8. Arun, R., Ashok, K.C.K., Sravanthi, V.V.N.S.S.: Cyclodextrins as drug carrier molecule: a review. Sci. Pharm. **76**, 567–598 (2008)

9. Davis, M.E., Brewster, M.E.: Cyclodextrin-based pharmaceutics: past, present and future. Nat. Rev. Drug Discov. **3**, 1023–1035 (2004)

10. Loftsson, T., Brewster, M.E.: Pharmaceutical applications of cyclodextrins: basic science and product development. J. Pharm. Pharmacol. **62**, 1607–1621 (2010)

11. Spulber, M., Pinteala, M., Fifere, A., Moldoveanu, C., Mangalagiu, I., Harabagiu, V., Simionescu, B.C.: Water soluble complexes of methyl-beta-cyclodextrin and sulconazole nitrate. J. Incl. Phenom. Macrocycl. Chem. **62**, 135–142 (2008)

12. Challa, R., Ahuja, A., Ali, J., Khar, R.K.: Cyclodextrins in drug delivery: an updated review. AAPS Pharm. Sci. Tech. **6**, 329–357 (2005)

13. Higuchi, T., Connors, K.A.: Phase-solubility techniques. Adv. Anal. Chem. Instrum. **4**, 117–122 (1965)

14. Domańska, U., Pelczarska, A., Pobudkowska, A.: Effect of 2-hydroxypropyl-β-cyclodextrin on solubility of sparingly soluble drug derivatives of anthranilic acid. Int. J. Mol. Sci. **12**, 2383–2394 (2011)

15. Lv, H.X., Zhang, Z.H., Jiang, H., Waddad, A.Y., Zhou, J.P.: Preparation, physicochemical characteristics and bioavailability studies of an atorvastatin hydroxypropyl-β-cyclodextrin complex. Pharmazie **67**, 46–53 (2012)

16. Hadžiabetdić, J., Elezović, A., Rahić, O., Mujezin, I.: Effect of cyclodextrin complexation on the aqueous solubility of diazepam and nitrazepam: phase-solubility analysis, thermodynamic properties. Am. J. Anal. Chem. **3**, 811–819 (2012)

17. Batt, D.K., Garala, K.C.: Preparation and evaluation of inclusion complexes of diacerein with β-cyclodextrin and hydroxypropyl β-cyclodextrin. J. Incl. Phenom. Macrocycl. Chem. **77**, 471–481 (2013)

18. George, S.J., Vasudevan, D.T.: Studies on preparation, characterization and solubility of 2-HP-beta-cyclodextrin-meclizine HCl inclusion complexes. Pharmaceutics **4**, 220–227 (2012)

19. Salústio, P.J., Feio, G., Figueirinhas, J.L., Pinto, J.F., Cabral Marques, H.M.: The influence of the preparation methods on the inclusion of model drugs in a beta-cyclodextrin cavity. Eur. J. Pharm. Biopharm. **71**, 377–386 (2009)

20. Patel, R., Patel, M.: Solid-state characterization and in vitro dissolution behavior of lorazepam: hydroxypropyl-β-cyclodextrin inclusion complex. Drug Discov. Ther. **4**, 442–452 (2010)

21. Petralito, S., Zanardi, I., Memoli, A., Annesini, M.C., Travagli, V.: Solubility, spectroscopic properties and photostability of rhein/cyclodextrin inclusion complex. Spectrochim. Acta. A. **74**, 1254–1259 (2009)

22. Dani, R.M.A.M., Elbashir, A.A.: Host-guest inclusion complex of β-cyclodextrin and cephalexin and its analytical application. Int. J. Pharm. Chem. Res. **2**, 1–13 (2013)

23. Marangoci, N., Mares, M., Silion, M., Fifere, A., Varganici, C., Nicolescu, A., Deleanu, C., Coroaba, A., Pinteala, M., Simionescu, B.C.: Inclusion complex of a new propiconazole derivative with beta-cyclodextrin: NMR, ESI-MS and preliminary pharmacological studies. Results Pharma. Sci. **1**, 27–37 (2011)

24. Cui, L., Zhang, Z.H., Sun, E., Jia, X.B.: Effect of beta-cyclodextrin complexation on solubility and enzymatic conversion of naringin. Int. J. Mol. Sci. **13**, 14251–14261 (2012)

25. Valnet, J., Duraffourd, C., Duraffourd, P., Lapraz, J.C.: L'aromatogramme: nouveaux resultats et essai d'interpretation sur 268 cas cliniques. Plant Médicin. Phytothér. **12**, 43–52 (1978)

26. Danciu, C., Soica, C., Oltean, M., Avram, S., Borcan, F., Csanyi, E., Ambrus, R., Zupko, I., Muntean, D., Dehelean, C.A., Craina, M., Popovici, R.A.: Genistein in 1:1 inclusion complexes with ramified cyclodextrins: theoretical, physicochemical and biological evaluation. Int. J. Mol. Sci. **15**, 1962–1982 (2014)

27. Malterud, K.E., Rydland, K.M.: Inhibitors of 15-lipoxygenase from orange peel. J. Agric. Food Chem. **48**, 5576–5580 (2000)

28. Hatano, T., Kagawa, H., Yasuhara, T., Okuda, T.: Two new flavonoids and other constituents in licorice root: their relative astringency and radical scavenging effects. Chem. Pharm. Bull **36**, 2090–2097 (1988)

29. Jullian, C., Moyano, L., Yañez, C., Olea-Azar, C.: Complexation of quercetin with three kinds of cyclodextrins: an antioxidant study. Spectrochim. Acta. A. **67**, 230–234 (2007)

30. Oyazu, M.: Studies on products of browning reactions: antioxidative activities of products of browning reaction prepared from glucosamine. Jpn. J. Nutr. **44**, 307–315 (1986)

31. Samal, H.B., Debata, J., Kumar, N.N., Sneha, S., Patra, P.K.: Solubility and dissolution improvement of aceclofenac using β-Cyclodextrin. Int. J. Drug Dev. Res. **4**, 326–333 (2012)

32. Dua, K., Pabreja, K., Ramana, M.V., Lather, V.: Dissolution behavior of β-cyclodextrin molecular inclusion complexes of aceclofenac. J. Pharm. Bioallied Sci. **3**, 417–425 (2011)

33. Calabro, M.L., Tommasini, S., Donato, P., Stancanelli, R., Raneri, D., Catania, S., Costa, C., Villari, V., Ficarra, P., Ficarra, R.: The rutin/β-cyclodextrin interactions in fully aqueous solution: spectroscopic studies and biological assays. J. Pharm. Biomed. Anal. **36**, 1019–1027 (2005)

34. Markham, K.R.: Techniques of flavonoid identification. Academic Press, New York (1982)

35. Connors, K.A.: Thermodynamics of pharmaceutical systems: an introduction for students of pharmacy. John Wiley & Sons Inc, Hoboken, New Jersey (2002)

36. Liu, B., Li, W., Nguyen, T.A., Zhao, J.: Empirical, thermodynamic and quantum-chemical investigations of inclusion complexation between flavanones and (2-hydroxypropyl)-cyclodextrins. Food Chem. **134**, 926–932 (2012)

37. Bloch, D.W., Elegakey, M.A., Speiser, P.P.: Solid dispersion of chlorthalidone in urea phase diagram and dissolution characteristics. Pharm. Acta Helv. **57**, 231–235 (1982)

38. Guo, X., Shuang, S., Wang, X., Dong, C., Pan, J., Aboul-Enein, H.Y.: Comparative study on the inclusion behaviour of cyclodextrin derivatives with venoruton and rutin by thin layer chromatography. Biomed. Chromatogr. **18**, 559–563 (2004)

39. Roik, N.V., Belyakova, L.A.: Thermodynamic, IR spectral and X-ray diffraction studies of the β-cyclodextrin-para-aminobenzoic acid inclusion complex. J. Incl. Phenom. Macrocycl. Chem. **69**, 315–319 (2011)

40. Lin, S.Y., Lin, H.L., Lin, C.C., Hsu, C.H., Wu T.K., Huang Y.T.: Thermodynamic study of grinding-induced loratadine inclusion complex formation using thermal analysis and curve-fitted FTIR determination. In: Moreno-Piraján, J.C. (ed.) Thermodynamics -

Physical Chemistry of Aqueous Systems (2011). doi: 10.5772/21338

41. Şamli, M., Korel, F., Bayraktar, O.: Characterization of silk fibroin based films loaded with rutin–β-cyclodextrin inclusion complexes. J. Incl. Phenom. Macrocycl. Chem. (2014). doi:10.1007/s10847-014-0396-4

42. Miron, L., Mares, M., Nastasa, V., Spulber, M., Fifere, A., Pinteala, M., Harabagiu, V., Simionescu, B.C.: Water soluble sulconazole-β-cyclodextrin complex: physico-chemical characterization and preliminary pharmacological studies. J. Incl. Phenom. Macrocycl. Chem. 63, 159–162 (2009)

43. Fatiha, M., Khatmi, D.E., Largate, L.: Theoretical approach in the study of the inclusion processes of sulconazole with β-cyclodextrin. J. Mol. Liq. 154, 1–5 (2010)

44. Piel, G., Dive, G., Ervard, B., Van Hees, T., Henry de Hassonville, S., Delattre, L.: Molecular modeling study of β- and γ-cyclodextrin complexes with miconazole. Eur. J. Pharm. Sci. 13, 271–279 (2001)

45. Grandelli, H.E., Stickle, B., Whittington, A., Kiran, E.: Inclusion complex formation of β-cyclodextrin and naproxen: a study on exothermic complex formation by differential scanning calorimetry. Incl. Phenom. Macrocycl. Chem. 77, 269–277 (2013)

46. Panda, S., Singh, D.L.: Study of antioxidant, antimicrobial and anthelmintic properties of 1-nicotinoyl-4-aryl-3-methyl 3a,4-dihydropyrazolo [3,4c] pyrazoles and their inclusion complexes with β-cyclodextrin. World J. Pharm. Pharm. Sci. 3, 1639–1654 (2014)

47. Stavniichuk, R., Drel, V.R., Shevalye, H., Vareniuk, I., Stevens, M.J., Nadler, J.L., Obrosova, I.G.: Role of 12/15-lipoxygenase in nitrosative stress and peripheral prediabetic and diabetic neuropathies. Free Radicals Biol. Med. 49, 1036–1045 (2010)

48. Wittwer, J., Hersberger, M.: The two faces of the 15-lipoxygenase in atherosclerosis. Prostaglandins Leukot. Essent. Fatty Acids 77, 67–77 (2007)

49. Yang, H., Zhuo, J.M., Chu, J., Chinnici, C., Praticò, D.: Amelioration of the Alzheimer's disease phenotype by absence of 12/15-Lipoxygenase. Biol. Psychiatry 68, 922–929 (2010)